ADVANCED FUNCTIONAL MATERIALS
www.afm-journal.de

Materials Views
www.MaterialsViews.com

Optical pH Sensor with Rapid Response Based on a Fluorescein-Intercalated Layered Double Hydroxide

By *Wenying Shi, Shan He, Min Wei,* David G. Evans,* and *Xue Duan*

The preparation of a highly oriented photoluminescent film of fluorescein (FLU) and 1-heptanesulfonic acid sodium (HES) co-intercalated in a layered double hydroxide (LDH) matrix by electrophoretic deposition (EPD) is reported, and its application as an optical pH sensor is demonstrated. The FLU-HES/LDH films with thickness ranging from nanometer to micrometer on indium tin oxide substrates exhibite good *c*-orientation of LDH platelets (the *ab*-plane of the LDH platelets parallel to the substrate), as confirmed by X-ray diffraction and scanning electron microscopy. Polarized luminescence of the film is observed with anisotropy value $r = 0.29$, resulting from the highly oriented FLU in the LDH gallery. Furthermore, the optical pH sensor with film thickness of 300 nm exhibits a broad linear dynamic range for solution pH (5.02–8.54), good repeatability (relative standard deviation (RSD) less than 1.5% in 20 consecutive cycles) and reversibility (RSD less than 1.5% in 20 cycles), high photostability and storage stability (ca. 95.2% of its initial fluorescence intensity remains after one month) as well as fast response time (2 s). Therefore, this work creates new opportunities for the preparation and application of LDH-based chromophores in the field of optical sensors.

1. Introduction

Optical pH sensors have become very popular analytical tools in the last decade,[1] due to their broad application in marine research,[2] blood measurement,[3] toxicological assay,[4] and biotechnology.[5] Generally, the fluorophore indicators are immobilized in a matrix for the purpose of obtaining optical pH sensors with stable lifetime and signal. Poor immobilization causes leaching of the indicator and drifting of the signal, resulting in the breakdown of its sensing ability in the extreme case.[6] Most optical pH indicators are immobilized in a suitable, proton-permeable, sol-gel polymer matrix.[7] However, some inherent demerits of polymers, such as relatively poor thermal or optical stability as well as toxicity, have limited the practical application of pH sensors to date. Therefore, it is essential to search for novel materials to immobilize the fluorophore indicator in order to achieve optical pH sensors with high stability and environmental compatibility.

[*] Dr. W. Y. Shi, Dr. S. He, Prof. M. Wei, Prof. D. G. Evans, Prof. X. Duan
State Key Laboratory of Chemical Resource Engineering
Beijing University of Chemical Technology
Beijing 100029 (P. R. China)
E-mail: weimin@mail.buct.edu.cn

DOI: 10.1002/adfm.201001081

Recently, considerable interest has been focused on the fabrication of chromophore–inorganic composite materials, since they may show novel functionalities (increased photo-, thermal, and mechanical stability) that are not present in the individual components alone.[8] Among inorganic matrices, layered double hydroxides (LDHs), whose structure can be generally expressed as $[M^{II}_{1-x}M^{III}_{x}(OH)_2](A^{n-})_{x/n}\cdot mH_2O$ (where M^{II} and M^{III} are divalent and trivalent metals, respectively, and A^{n-} is an n-valent anion), are one type of important layered materials that display a large versatility in terms of their chemical composition and the ability to build up 2D-organized structures (stacking of the layers giving rise to an accessible interlayer space on the nanometer scale).[9] The incorporation of chromophores into the LDH gallery exhibits the following advantages: first, the LDH matrix provides chromophore molecules with a confined and stable environment, which reduces molecular thermal agitation (intermolecular collisions, vibrations, and rotations, etc.) and improves fluorescence efficiency; second, chromophore aggregation in the LDH matrix is effectively inhibited by host–guest interactions (e.g., electrostatic attraction, hydrogen bonding), and fluorescence quenching is therefore reduced; third, chromophore molecules immobilized in the LDH matrix exhibit optical and thermal stability, environmental compatibility, and low operational risk.

In recent years, LDH thin films have attracted great attention for potential applications in catalysis, adsorption, chemical sensors, and fluorescent materials. Many preparation methods of LDH thin films have been reported. Gardner et al.[10] found that colloidal LDH suspensions obtained by hydrolysis of alkoxide-intercalated LDH derivatives were able to form transparent films. Lee et al.[11] used ultrasonification to prepare monolayers of LDH films with a high packing density, whilst Liu, Li, and coworkers[12] reported that the exfoliation of LDH gives colloidal LDH particles, which can be used as building blocks in the preparation of ultrathin films by the layer-by-layer technique. Our group[13] has recently reported fabrication of NiAl-LDH film by an in situ growth technique on porous anodic alumina/aluminum (PAO/Al) substrates. The electrophoretic deposition (EPD) method, achieved by the motion of charged particles towards an oppositely charged surface due to an external applied electric field, shows a wide range of novel applications

in fabricating biological sensors, energy conversion, and optical coatings and devices.[14] This technique has recently gained in interest due to its simplicity in equipment setup (shown in Figure S1 in the Supporting Information), low cost, high deposition rate, ease of thickness control, and strong adherence to substrates.[15] Therefore, the EPD technique provides a new method for the assembly of LDH films.

Fluorescein (FLU),[16] with large extinction coefficient, high quantum yield, and biological tolerance, is one of the most extensively studied fluorescence indicators in pH sensor applications.[17] Its absorption and fluorescence properties strongly depend on pH value owing to the presence of cationic, neutral, and anionic forms in aqueous solution.[18] In our previous work,[19] the orientation of α-naphthalene acetate and its fluorescence properties in the galleries of a Zn_2 Al LDH were studied. In this paper, we further report a highly oriented photoluminescence film through co-intercalation of FLU and a surfactant (1-heptanesulfonic acid sodium, HES) into a Mg_2Al-LDH matrix by the EPD method, and demonstrate its application as an optical pH sensor. The highly oriented FLU-HES/LDH films with thickness ranging from nanometer to micrometer on indium tin oxide (ITO) substrates were obtained by the EPD method. Polarized luminescence of the film was observed with anisotropy value $r = 0.29$, resulting from the highly oriented FLU in the LDH gallery. Furthermore, the optical pH sensor with a film thickness of 300 nm exhibits a broad linear dynamic range for solution pH (5.02–8.54), good repeatability (relative standard deviation (RSD) less than 1.5% in 20 consecutive cycles) and reversibility (RSD less than 1.5% in 20 cycles), high photostability and storage stability (ca. 95.2% of its initial fluorescence intensity remains after one month) as well as fast response time (2 s). Therefore, the novel strategy in this work not only provides a method for fabrication of highly oriented luminescence films with precise control of thickness (ranging from nanometers to micrometers) by the EPD method, but also demonstrates its prospective application in the field of optical pH sensors.

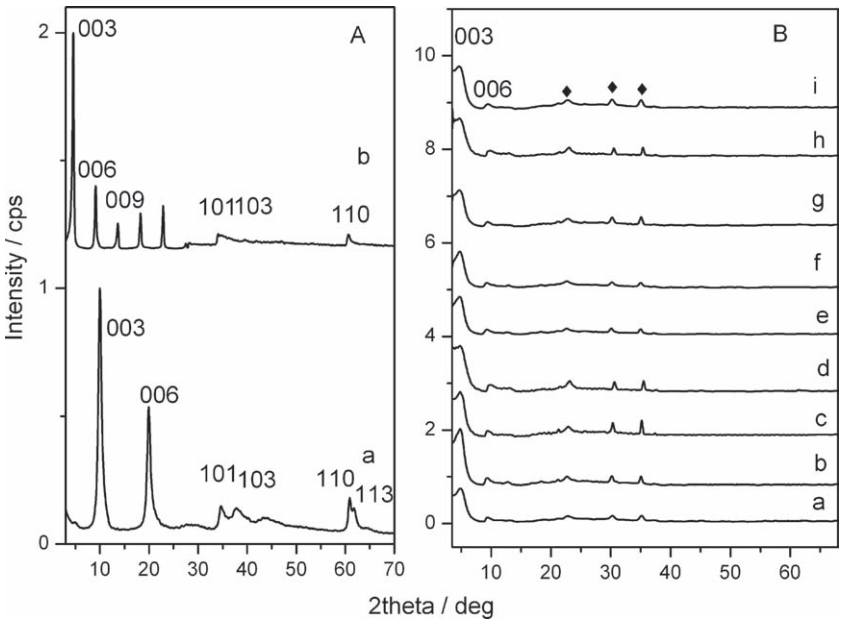

Figure 1. A) XRD patterns of powder samples for a) Mg_2Al-NO_3 LDH and b) FLU-HES/LDH. B) XRD patterns for the FLU-HES/LDH thin-film samples with different electrophoresis times: a–i) t = 1, 2, 3, 6, 7, 9, 10, 20, and 30 min, respectively. "♦" denotes reflections from the ITO substrate.

2. Results and Discussion

2.1. Macroscopic Orientation and Tunable Thickness of the FLU-HES/LDH Thin Films

The X-ray diffraction (XRD) patterns of Mg_2Al-NO_3 LDH and FLU-HES/LDH are shown in **Figure 1**. All the patterns of these samples can be indexed to a hexagonal lattice. The interlayer spacing can be calculated by averaging the positions of the three harmonics: $c = (1/3)(d_{003} + 2d_{006} + 3d_{009})$. The 003 reflection of the Mg_2Al-NO $_3$ LDH powder sample at $2\theta = 9.9°$ (Figure 1A, curve a) shows an interlayer distance of 0.88 nm. The XRD patterns of Mg_2Al-NO_3 LDH and FLU-HES/LDH (x = 1.00×10^{-3}%, 5.00×10^{-3}%, 1.25×10^{-2}%, 2.00×10^{-2}%, and 4.00×10^{-2}%) are shown in Figure S2. The basal spacing of FLU-HES/LDH (x) (Figure S2B, curves a–f) increases from 1.58 nm ($x = 0$) to 1.94 nm ($x = 4.00 \times 10^{-2}$%), indicating that FLU and HES were co-intercalated into the galleries of the LDH. The variation of the basal spacing can be attributed to the different arrangements of interlayer guest molecules resulting from different ratios of FLU/HES. Moreover, the half-peak width (full width at half the maximum, FWHM) of the 003 reflection (0.28°–0.38°) for all the FLU-HES/LDH (x) samples (Figure S2B) is less than that of the precursor Mg_2Al-NO_3 LDH (0.75°) (Figure S2A), that is, no broadening of 003 reflection occurs after co-intercalation of FLU and HES. In addition, a good linear relationship between d_{003} and x in the x range 1.00×10^{-3}% –4.00×10^{-2}% (Figure S3) was observed with a low error (≤3%). The above results indicate that FLU is solubilized in the HES phase and forms a homogeneous phase in the interlayer of LDH.

Compared with the FLU-HES/LDH powder sample (Figure 1A, curve b), it can be seen that the FLU-HES/LDH thin films (electrophoresis time t = 1, 2, 3, 6, 7, 9, 10, 20, and 30 min; Figure 1B, curves a–i) show only one series of 00l reflections, indicating a highly ordered stacking of the ab plane of LDH platelets parallel to the substrate. Figure S4 shows scanning electron microscopy (SEM) side-view images of the FLU-HES/LDH films, from which a linear correlation between film thickness and electrophoretic time was obtained ($R = 0.9998$, shown in Figure S5). The Fourier transform infrared (FTIR) spectra further confirmed the co-intercalation of the two anions (see Figure S6). Moreover, the FLU and HES co-intercalated

LDH composites showed favorable luminescence properties with FLU/HES ratio in the range 10^{-4}–10^{-3} (Figure S7). As a result, the sample with ratio FLU/HES = 2×10^{-4} was chosen for further study in this work. The chemical composition is $[Mg_{0.67}Al_{0.33}(OH)_2](FLU)_{6.60\times10^{-5}}(HES)_{0.329} \cdot 0.51H_2O$ based on the elemental analysis results, indicating that the experimental ratio of FLU/HES in the FLU-HES/LDH composite is close to the nominal ratio, as expected.

The FLU-HES/LDH (t) thin films were fabricated to test their feasibility as a pH sensor. Figures S8 and S9 show the absorption spectra and response time, respectively, of the thin films with different thicknesses from 100 to 600 nm (1 min ≤ t ≤ 6 min). It was found that both absorption intensity and response time increased when the thickness of the FLU-HES/LDH thin film was increased. The enhancement in absorption intensity results from the increase of FLU amount, whereas the increase in response time is related to the reduced diffusion rate of OH^- or H^+ in the film with larger thickness. Taking into account both the absorption intensity and response time, the FLU-HES/LDH (300 nm, t = 3 min) thin film sample was chosen in the following study. The SEM image of the FLU-HES/LDH (t = 3 min) thin film exhibits an extraordinarily smooth and continuous surface in the top view (**Figure 2A**). High magnification of the film (Figure 2B) demonstrates that the FLU-HES/LDH nanoplatelets (100–200 nm) are densely packed on the substrate plane with good *c*-orientation, consistent with the XRD results in Figure 1. Furthermore, the fluorescence microscopy image shows a homogeneous brightness of green light (Figure 2C), demonstrating a uniform distribution of the FLU chromophore throughout the film.

2.2. Fluorescence Properties of the FLU-HES/LDH (t = 3 Min) Thin Film

2.2.1. Fluorescence Lifetime of FLU

The lifetime of the fluorophore indicator is a crucial parameter in the evaluation of an optical pH sensor. A FLU solution in water/ethanol (1:1, v/v; FLU: 10^{-5} mol L^{-1}; HES: 0.05 mol L^{-1}) and FLU-HES/LDH powder and film samples were studied by detecting their fluorescence decays with excitation and emission wavelengths of 490 and 510 nm, respectively. The fluorescence lifetimes were obtained by fitting the decay profiles with one-exponential and double-exponential forms (**Table 1**); the fitting results obtained from the double-exponential function is better (based on the χ^2 value). Multiexponential decay curves were usually observed in solid samples and can be attributed to highly heterogeneous environments for the molecules in the solid surfaces.[20] A similar conclusion has been reported by other researchers studying intercalation of Rhodamine 6G (R6G) into Laponite clay.[21] It can be observed from Table 1 that the emission lifetime of the FLU-HES/LDH powder sample (2.21 ns) is significantly longer than that of FLU in solution (1.80 ns). This result indicates that the confinement effect imposed by the LDH matrix decreases the radiationless decay rate constant and thus increases the fluorescence lifetime of FLU. The lifetime of FLU in solution in this work is shorter than that of previous reports,[21a,22] which is related to the solvent effect and media effects. In addition, a longer fluorescence lifetime of the film sample (2.56 ns) compared to the powder sample (2.21 ns) was obtained, indicating that the confinement effect was further enhanced after the formation of the film with a highly ordered stacking of the *ab*-plane of LDH platelets parallel to the substrate.

Table 1. Fluorescence decay data of FLU in solution and the FLU-HES/LDH samples [a].

Samples	n	τ_i [ns]	A_i [%]	$<\tau>$ [ns]	χ^2
Powder	1	2.02	100		1.30
	2	0.78	59.6	2.21	1.25
		4.31	40.4		
Film	1	2.38	100		1.26
	2	1.06	56.4	2.56	1.14
		4.52	43.6		
Solution [10^{-5} mol L^{-1}]	1	1.80	100	1.80	1.22

[a] n is the power of the exponential fit; τ_i is the fluorescence lifetime; A_i is the pre-exponential factor related to the statistical weights of each exponential; $<\tau>$ is the intensity average lifetime. The goodness of fit is indicated by the value of χ^2.

2.2.2. Steady-State Fluorescence Polarization

One of the most common methods of evaluating fluorescence polarization is the measurement of the anisotropy r value, which was fully described by Valeur.[23] r can be expressed by

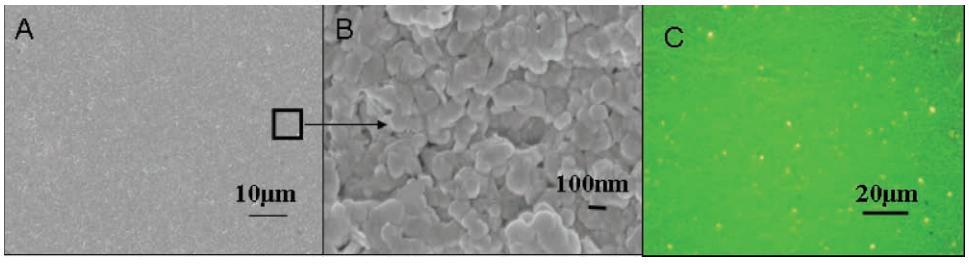

Figure 2. SEM images of the FLU-HES/LDH (t = 3 min) thin film at A) low magnification and B) high magnification. C) Fluorescence microscopy image of the FLU-HES/LDH (t = 3 min) thin film.

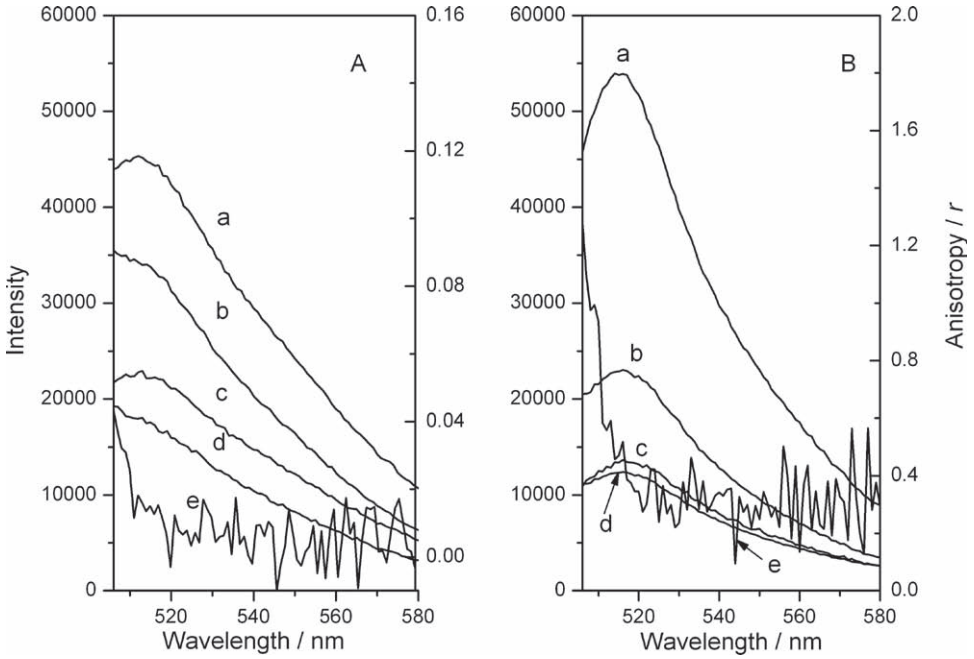

Figure 3. Photoemission profiles in the a) HH, b) HV, c) VH, d) VV, and e) polarizations and anisotropy of a FLU-HES/LDH sample measured at room temperature (293 K): A) powder, B) thin film (t = 3 min). The excitation wavelength is 490 nm.

$$r = \frac{I_{\parallel} - I_{\perp}}{I_{\parallel} + 2I_{\perp}} \text{ or } r = \frac{I_{VV} - G I_{VH}}{I_{VV} + 2G I_{VH}} \quad (1)$$

where $I_{\parallel}$ and $I_{\perp}$ are the photoluminescence intensity measured in the planes parallel and perpendicular to the excitation radiation, respectively ($G \equiv I_{HV}/I_{HH}$); I_{VH} is the photoluminescence intensity obtained with vertical excitation polarization and horizontal detection polarization; I_{VV}, I_{HV}, and I_{HH} are defined in a similar way. Theoretically, the value of r is in the range from –0.2 (absorption and emission transition dipoles perpendicular) to 0.4 (two transition dipoles parallel), and deviation from these values means a reorientation of the emission dipole moment.

The polarized photoemission spectra of the FLU-HES/LDH powder and film samples are displayed in **Figure 3**. It was found that the anisotropic value of the FLU-HES/LDH powder sample is 0.01, whereas it is ca. 0.29 for the film sample. This result indicates that the highly ordered orientation of LDH platelets leads to enhanced anisotropy of the film sample.

2.3. The FLU-HES/LDH (t = 3 Min) Thin Film as an Optical pH Sensor

2.3.1. The pH Response

Figure 4A shows that the fluorescence intensity of the FLU-HES/LDH (t = 3 min) thin film increases as the pH value increases from 4.01 up to 12.01. The titration plots of this film as well as the FLU solution (10^{-5} mol L^{-1}) obtained with excitation of 490 nm and emission of 516 nm are displayed in Figure 4B. As the pH value increases, the emission intensity of the FLU solution increases gradually and reaches a constant at pH 7.8 with an approximately linear response in the pH range 5.51–7.54. FLU displays a complex pH-dependent equilibrium resulting from its various ionic forms (Figure S10),[24] but only anionic forms (monoanion and dianion) are fluorescent. Therefore the change in fluorescence intensity is based on the equilibrium between the two fluorescent forms of FLU. For the FLU-HES/LDH (t = 3 min) thin film, the emission intensity and brightness (Figure S11) increase gradually along with the increase of pH value, similar to the FLU solution. However, a much broader linear response range (pH 5.02–8.54) as well as a higher sensitivity than FLU solution were obtained.

In order to obtain further insight into the pH response of the sensor, pK_a of FLU solution and the FLU-HES/LDH (t = 3 min) thin film was calculated according to[25]

$$pK_a = \frac{pH - \log(S_x - S_a)}{S_b - S_x} \quad (2)$$

where S_x, S_a, and S_b are the fluorescence intensity corresponding to a defined pH within the titration plot, the acid form, and the base form, respectively.

The pK_a of the FLU-HES/LDH (t = 3 min) thin film (6.92) is larger than that of FLU solution (6.65), which leads to a significant broadening of the titration plot (a wider dynamic range; see Figure 4B).[26] Actually, host–guest interactions between the LDH matrix and FLU (e.g., electrostatic attraction, hydrogen bonding) exert an effect on pK_a and thus the dynamic range. This can be confirmed by the results of attenuated total reflection (ATR) FTIR spectroscopy for the FLU-HES/LDH thin film (t = 3 min) (Figure S12). It was found that both the C=O stretching of FLU[27] and the O–H stretching absorption belonging to water molecules adsorbed on the LDH layer shifted to higher frequency — from 1590 to 1607 cm^{-1}

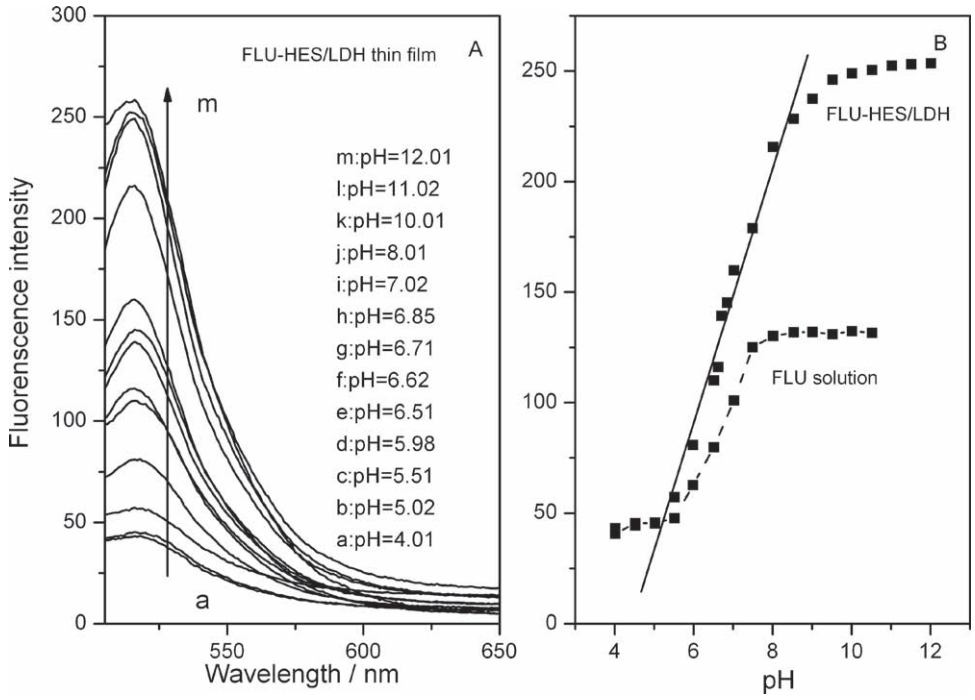

Figure 4. A) Emission spectra of the FLU-HES/LDH (t = 3 min) thin film at different pH values (295 K, I = 0.02 M HNO_3 and NaOH, λ_{ex} = 490 nm). B) pH titration curves for the FLU-HES/LDH (t = 3 min) thin film and FLU solution.

and from 3295 to 3310 cm^{-1}, respectively — as pH value increased from 5.5 to 11.5, indicating that the increase of pH led to enhancement of the hydrogen bonding interaction between FLU and LDH layer and consequently a wider dynamic response range. In addition, the absorption spectra of the FLU-HES/LDH (t = 3 min) thin film at different pH values (Figure S13) agree with the results of fluorescence spectra. Therefore, the FLU-HES/LDH (t = 3 min) thin film can be used as a pH sensor in a broad linear response range (from 5.02 to 8.54), which is relevant for many biological, environmental, and physiological applications.

2.3.2. Repeatability and Reversibility

It is widely known that the main drawback of pH sensors based on immobilized dye on a sol-gel is the leaching of the dye over prolonged periods, leading to unreproducible measurements.[28] In this work, the pH sensor was measured in solution with pH 5.02, 6.51, and 8.54, and the fluorescence intensity at the maximum emission peak was recorded (**Figure 5A**). The results show that no obvious signal drift was observed, and good repeatability over 20 consecutive cycles was obtained with RSD of 1.41% (pH 5.02), 0.65% (pH 6.51), and 0.84% (pH 8.54). The reversibility of the pH sensor was studied by alternate immersion into two solutions with pH 5.02 and 8.54 (Figure 5B). The RSD of 20 cycles was 1.37% (pH 5.02) and 1.35% (pH 8.54). In addition, no trace of leached FLU was detected in the measured solution. The storage stability test of the sensor shows that ca. 95.2% of its initial fluorescence intensity remains after one month (Figure S14). Therefore, the pH sensor modified by the FLU-HES/LDH (t = 3 min) thin film possesses good repeatability, reversibility, and storage stability, owing to the confinement effect of the LDH matrix on the intercalated FLU species.

2.3.3. Photostability

The photostability of a pH sensor is of major importance, since poor stability leads to the irreversible loss of fluorescence, which limits the statistical accuracy of the detection in biological, environmental, and physiological applications.[29] The fluorescence intensity of FLU in solution and FLU-HES/LDH powder and film were recorded by illuminating them with UV light in a comparative study. **Figure 6** displays the fluorescence intensity of these samples as a function of bleaching time. It was found that the half-life of the FLU-HES/LDH powder sample (5.5 h) was more than twice that of the FLU solution (2.5 h). This indicates that the confined environment in the rigid LDH matrix improves the photostability of the FLU molecule significantly. FLU molecules were uniformly distributed in the LDH matrix by the surfactant molecules, and thus fluorescence quenching was reduced effectively. In addition, the photostability of FLU-HES/LDH was further enhanced through the formation of the film (half-life of 6 h), due to the ordered and compact stacking of the LDH platelets. Furthermore, as shown in Figure S15, no delamination or peeling occurred on cross-cutting the surface, indicating strong adherence of the film to the substrate. The above results show that the pH sensor prepared by EPD possesses high photostability and mechanical stability.

2.3.4. The Response Time

The response time of the pH sensor was defined as the so-called t_{95} time in this work, which is the time taken for intensity

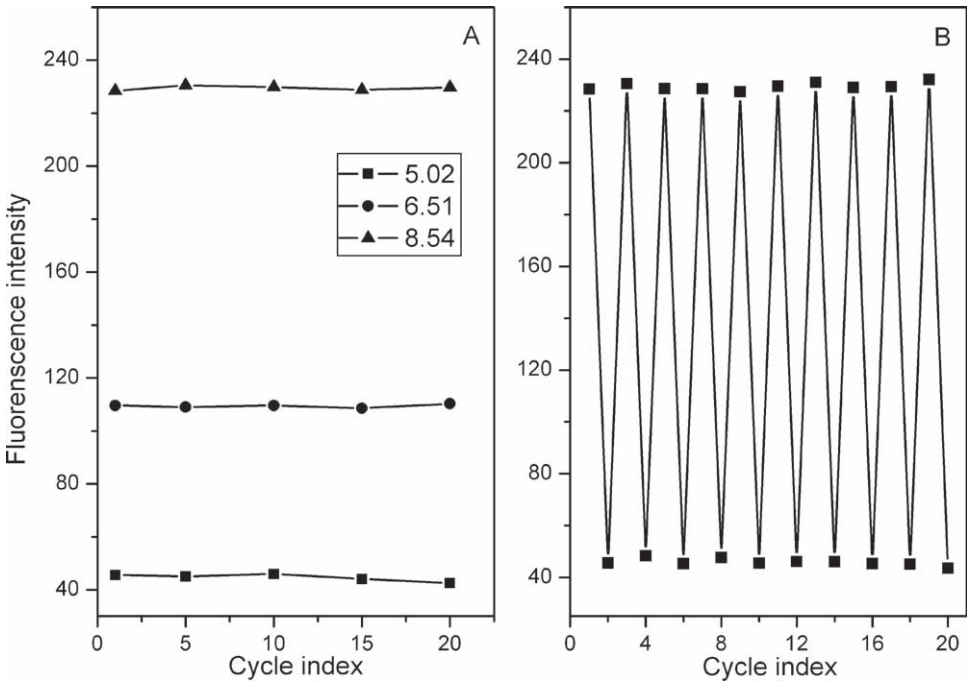

Figure 5. A) Fluorescence intensity of the pH sensor recorded after 1, 5, 10, 15, and 20 cycles at pH 5.02, 6.51, and 8.54. B) The reversibility recorded by alternate measurement in two solutions with pH 5.02 and 8.54.

to reach 95% of the final value when the pH value is changed. It was measured by exposing the pH sensor to solutions with different pH from low to high (pH 5.02, 6.51, and 8.54) with a holding time of 10 s and then reversing the manipulation. The response time was 2 s in both directions (**Figure 7**), which is a key feature for the practical application of the pH sensor. The fast response time is possibly related to the nanometer scale of the FLU-HES/LDH particles (Figure 2B), which is favorable for mass transfer and diffusion. It has been reported that a nonlinear response of pH sensors is commonly observed in systems with a polymer as the matrix, owing to the pH-dependent swelling behavior.[30] In this work, however, the pH sensor consisting of FLU-HES/LDH thin film exhibits a wide linear range with high sensitivity and fast response, owing to the immobilization of FLU in a confined 2D environment imposed by inorganic LDH.

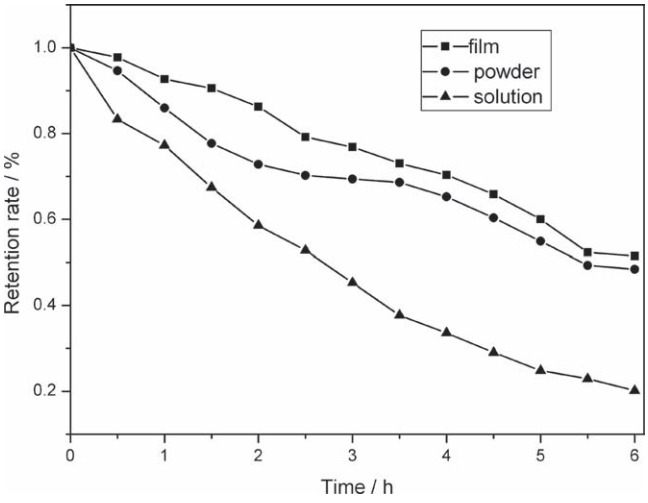

Figure 6. The photostability of the FLU-HES/LDH (t = 3 min) thin film, powder and FLU solution as a function of bleaching time. Indicated values are means of three experiments with standard error less than 3%.

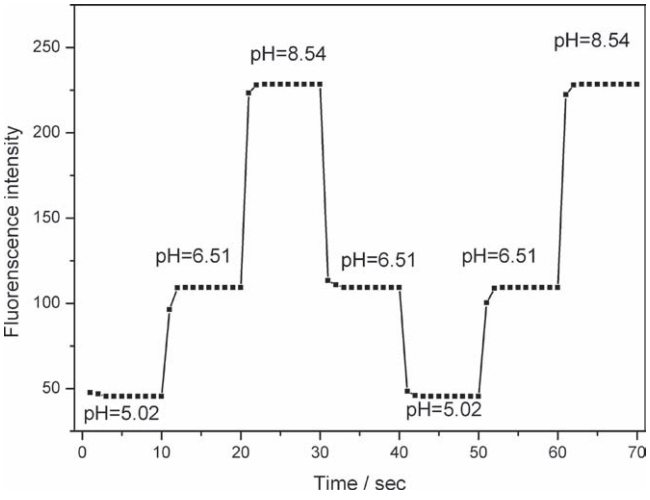

Figure 7. Response time of the pH sensor recorded by fluorescence intensity at the maximum emission peak. The interval between each measurement is 1 s and the excitation wavelength is 490 nm. Indicated values are means of three experiments with RSD less than 0.8%.

3. Conclusions

FLU and HES were co-intercalated between sheets of Mg_2Al LDH by anion exchange, and thin films of FLU-HES/LDH with good *c*-orientation verified by XRD and SEM were obtained by EPD on ITO substrates. It was found that the FLU-HES/LDH thin films show a longer lifetime than the corresponding powder sample. The anisotropy of the film was observed by fluorescence polarization, which can be attributed to the highly oriented FLU in the LDH gallery. An optical pH sensor with film thickness of 300 nm was obtained, which shows a broad linear dynamic range for solution pH, good repeatability and reversibility, high photostability and storage stability as well as fast response time. Therefore, this work provides a method for fabrication of highly oriented luminescent film with precise control of thickness (ranging from nanometer to micrometer). It is anticipated that this method for the assembly of LDH films will create new opportunities for the preparation and application of LDH-based chromophores in the field of optical sensors.

4. Experimental Section

Chemicals: Sodium FLU and HES (biochemistry grade) were purchased from Sigma-Aldrich Company. Analytical grade chemicals, including $Mg(NO_3)_2{\cdot}6H_2O$, $Al(NO_3)_3{\cdot}9H_2O$, NaOH, C_2H_5OH, and HNO_3, were purchased from the Beijing Chemical Co. Limited and used without further purification. Deionized and decarbonated water was used in all experimental processes.

Synthesis of the FLU-HES/LDH Colloid Suspension: The Mg_2Al-NO_3LDH precursor was synthesized by the hydrothermal method.[31] Subsequently, the FLU and HES co-intercalated LDH colloid composite was prepared following the ion-exchange method. FLU (2×10^{-6} mol) and HES (10^{-2} mol) were dissolved in 150 mL of water/ethanol mixture solvent (1:1, v/v). Freshly prepared Mg_2Al-NO_3LDH colloid (40 mL) was dispersed in the mixture solution thoroughly. The suspension was agitated at room temperature under N_2 atmosphere for 48 h. The FLU-HES/LDH colloid suspension was obtained by washing it extensively with water and then dispersing in ethanol (Figure S16).

Fabrication of the FLU-HES/LDH Thin Films: Substrates of ITO were first cleaned by immersing them in deionized water and ethanol in an ultrasonic bath for 30 min. The thin film of FLU-HES/LDH was fabricated by EPD (a schematic illustration of the setup is shown in Figure S1).[32] Ethanol was used as a dispersion medium to prepare the colloidal nanoparticle suspension of FLU-HES/LDH (10^{-3} mol L^{-1}). Two ITO substrates were used as the working and counter electrodes, which were placed parallel to each other with a separation of 1 cm. The voltage between the two electrodes was set at 9 V and the thickness of the film can be precisely controlled by changing the electrophoretic time.

Measurement of pH Response: Solutions with different pH values were prepared by adding 0.02 M NaOH or 0.02 M HNO_3 to 0.1 M $NaNO_3$ (295 K) solution and measured using a pH meter (Mettler Toledo Co., Switzerland). The response of the pH sensor was recorded by RF-5301PC fluorophotometer with a liquid holder. The pH sensor was immersed in a quartz cell with pH solution. Between two different pH measurements the pH sensor was washed thoroughly with deionized and decarbonated water.

Techniques of Characterization: The powder XRD measurements were performed on a Rigaku XRD-6000 diffractometer, using Cu Kα radiation ($\lambda = 0.15418$ nm) at 40 kV, 30 mA, with a scanning rate of 2° min^{-1}, and a 2θ angle ranging from 2° to 70°. SEM images were obtained using a Zeiss scanning electron microscope. The UV-vis spectra were collected in a Shimadzu U-3000 spectrophotometer. Fluorescence emission spectra were recorded on a RF-5301PC fluorophotometer (1.5 nm resolution) in the range 500–650 nm with an excitation wavelength of 490 nm and slit widths of 3 nm. Elemental analysis samples were prepared by dissolving 30 mg of solid sample in a few drops of concentrated HNO_3 and diluting this to 50 mL with water. Mg and Al elemental analysis was performed by atomic emission spectroscopy with a Shimadzu ICPS-7500 instrument. C, H, N content was determined using an Elementar vario elemental analysis instrument. The water content of the sample was obtained by thermogravimetry. The FLU content was determined by quantitative analysis of fluorescence with a RF-5301PC fluorophotometer. Fluorescence was observed using an Olympus BX51 fluorescence microscope. The photobleaching was tested under UV illumination with CHF-XQ 500W. Steady-state polarized photoluminescence measurements were recorded with an Edinburgh Instruments' FLS 920 fluorimeter. The lifetime was measured by exciting the samples at 490 nm with a nanosecond flashlamp. The response time was recorded at intervals of 1 s by the RF-5301PC fluorophotometer with the time course model.

Supporting Information

Supporting Information is available from the Wiley Online Library or from the author.

Acknowledgements

This project was supported by the National Natural Science Foundation of China, the 111 Project (Grant No.: B07004), the 973 Program (Grant No.: 2009CB939802) and the Fundamental Research Funds for the Central Universities (Grant No.: ZZ0908).

Received: May 28, 2010
Published online: August 27, 2010

[1] a) O. S. Wolfbeis, *J. Mater. Chem.* **2005**, *15*, 2657; b) L. A. Perelman, T. Moore, J. Singelyn, M. J. Sailor, E. Segal, *Adv. Funct. Mater.* **2010**, *20*, 826; c) M. Michelle, M. Ward, S. A. Asher, *Adv. Funct. Mater.* **2008**, *18*, 1186.
[2] a) H. Stahl, A. Glud, C. R. Schröder, I. Klimant, A. Tengberg, R. N. Glud, *Limnol. Oceanogr.: Meth.* **2006**, *4*, 336; b) C. R. Schroeder, B. M. Weidgans, I. Klimant, *Analyst* **2005**, *130*, 907.
[3] S. A. Grant, R. S. Glass, *Sens. Actuators B* **1997**, *45*, 35.
[4] S. Arain, G. T. John, C. Krause, J. Gerlach, O. S. Wolfbeis, I. Klimant, *Sens. Actuators B* **2006**, *113*, 639.
[5] a) Y. Kostov, P. Harms, L. R. Eichhorn, G. Rao, *Biotechnol. Bioeng.* **2001**, *72*, 346; b) G. T. John, D. Goelling, I. Klimant, H. Schneider, E. Heinzle, *J. Dairy Res.* **2003**, *70*, 327; c) A. Zanzotto, N. Szita, P. Boccazzi, P. Lessard, A. J. Sinskey, K. F. Jensen, *Biotechnol. Bioeng.* **2004**, *87*, 243; d) Z. Zhang, N. Szita, P. A. Boccazzi, J. Sinskey, K. F. Jensen, *Biotechnol. Bioeng.* **2006**, *93*, 286.
[6] M. Uttamlal, W. D. Sloan, D. Millar, *Polym. Int.* **2002**, *51*, 1198.
[7] J. Lin, *Trends Anal. Chem.* **2000**, *19*, 541.
[8] a) L. Latterini, M. Nocchetti, G. G. Aloisi, U. Costantino, F. Elisei, *Inorg. Chim. Acta* **2007**, *360*, 728; b) J. Bauer, P. Behrens, M. Speckbacher, H. Langhals, *Adv. Funct. Mater.* **2003**, *13*, 241; c) P. L. Gentili, U. Costantino, R. Vivani, L. Latterini, M. Nocchetti, G. G. Aloisi, *J. Mater. Chem.* **2004**, *14*, 1656; d) H. P. Cong, S. H. Yu, *Adv. Funct. Mater.* **2007**, *17*, 1814; e) H. Kakiuchida, M. Takahashi, Y. Tokuda, T. Yoko, *Adv. Funct. Mater.* **2009**, *19*, 2569.
[9] a) G. R. Williams, D. O'Hare, *J. Mater. Chem.* **2006**, *16*, 3065; b) A. C. D. Newmann, *Chem. Clays Clay Miner.*, Longman Science Technology Mineral Society, London **1987**; c) O. H. Van, *An Introduction to Clay Colloid Chemistry*, Wiley, New York **1977**; d) J. Bauer, P. Behrens, M. Speckbacher, H. Langhals,*Adv. Funct. Mater.* **2003**,

13, 241; e) F. Millange, R. I. Walton, L. Lei, D. O'Hare, *Chem. Mater.* **2000**, *12*, 1990. f) A. M. Fogg, G. R. Williams, R. Chester, D. O'Hare, *J. Mater. Chem.* **2004**, *14*, 2369.

[10] E. Gardner, K. M. Huntoon, T. J. Pinnavaia, *Adv. Mater.* **2001**, *13*, 1263.

[11] a) J. H. Lee, S. W. Rhee, D. Y. Jung, *Chem. Mater.* **2004**, *16*, 3774; b) J. H. Lee, S. W. Rhee, D. Y. Jung, *Chem. Mater.* **2006**, *18*, 4740.

[12] a) L. Li, R. Z. Ma, Y. Ebina, K. Fukuda, K. Takada, T. Sasaki, *J. Am. Chem. Soc.* **2007**, *129*, 8000; b) Z. P. Liu, R. Z. Ma, M. Osada, N. Iyi, Y. Ebina, K. Takada, T. Sasaki, *J. Am. Chem. Soc.* **2006**, *128*, 4872.

[13] H. Y. Chen, F. Z. Zhang, S. S. Fu, X. Duan, *Adv. Mater.* **2006**, *18*, 3089.

[14] a) P. Sarkar, P. S. Nicholson, *J. Am. Ceram. Soc.* **1996**, *79*, 1987; b) R. Moreno, B. Ferrari, *Am. Ceram. Soc. Bull.* **2000**, *79*, 44; c) K. Kanamura, J. Hamagami, T. Umegaki, *Trans. Mater. Res. Soc. Jpn.* **2002**, *27*, 67; d) I. Zhitomirsky, *Adv. Colloid Interface Sci.* **2002**, *97*, 279.

[15] T. Takahiro, K. Yoji, H. Hideo, Y. Yoshinori, K. Nobuhiro, K. Nobukazu, E. M. Thomas, *J. Am. Chem. Soc.* **2006**, *128*, 16634.

[16] a) D. C. Neckers, A. O. M. Valdes, in *Advances in Photochemistry*, Vol. *18* (Eds: D. Volman, G. S. Hammond, D. C. Neckers), Wiley, New York, **1993**. b)C. S. Owen, *Anal. Biochem.* **1992**, *204*, 65. c) C. H. Tung, *Biopolymers* **2004**, *76*, 391; d) J. P. Taquet, C. Frochot, V. Manneville, H. M. Barberi, *Curr. Med. Chem.* **2007**, *14*, 1673; e) Y. P. Wang, P. Han, H. Xu, Z. Q. Wang, X. Zhang, A. V. Kabanov, *Langmuir* **2010**, *26*, 709.

[17] a) S. Ohkuma, B. Poole, *Proc. Natl. Acad. Sci.* USA **1978**, *5*, 3327; b) J. A. Thomas, R. N. Buchsbaum, A. Zimniak, E. Racker, *Biochemistry* **1979**, *18*, 2210.

[18] R. Sjoback, J. Nygren, M. Kubista, *Spectrochim. Acta, Part A* **1995**, *51*, L-7.

[19] W. Y. Shi, M. Wei, J. Lu, D. G. Evans, X. Duan, *J. Phys. Chem. C* **2009**, *113*, 12888.

[20] a) K. Rurack, K. Hoffman, W. Al-Soufi, G. U. Resch, *J. Phys. Chem. B* **2002**, *106*, 9744; b) L. Latterini, M. Nocchetti, G. G. Aloisi, U. Costantino, F. C. D. Schryver, F. Elisei, *Langmuir* **2007**, *23*, 12337.

[21] a) J. R. Lakowicz, *Principles of Fluorescence Spectroscopy*, 3rd ed., Springer Verlag, Berlin Heidelberg **2006**; b) B. Valeur, *Molecular Fluorescence: Principles and Applications*, Wiley-VCH, Weinheim, Germany **2002**; c) M. V. Martínez, A. F. López, P. J. Banuelos, A. I. López, *J. Phys. Chem. B* **2005**, *109*, 7443.

[22] a) M. Montalti, A. Credi, L. Prodi, M. T. Gandolfi, *Handbook of Photochemistry*, CRC, Boca Raton, FL **2006**; b) D. Magde, R. Wong, P. G. Seybold, *Photochem. Photobiol.* **2002**, *75*, 327; c) J. R. Unruh, G. Gokulrangan, G. S. Wilson, C. K. Johnson, *Photochem. Photobiol.* **2005**, *81*, 682. d) D. Magde, G. E. Rojas, P. G. Seybold, *Photochem. Photobiol.* **1999**, *70*, 737.

[23] B. Valeur, *Molecular Fluorescence: Principles and Applications*, Wiley-VCH, Weinheim **2001**.

[24] a) J. Yguerabide, E. Talavera, J. M. Alvarez, B. Quintero, *Photochem. Photobiol.* **1994**, *60*, 435; b) R. P. Haugland, *Handbook of fluorescent probes and reseach chemicals*, Molecular Probes Inc., Eugene, OR **1996**, p. 551; c) M. M. F. Choi, *J. Photochem. Photobiol. A: Chem.* **1998**, *114*, 235.

[25] L. Aleksandra, O. Ines, M. Ivana, S. W. Otto, *Anal. Chim. Acta* **1998**, *367*, 159.

[26] a) J. E. Lee, S. S. Saavedra, *Anal. Chim. Acta* **1994**, *285*, 265; b) S. C. Kraus, R. Czolk, J. Reichert, H. J. Ache, *Sens. Actuators, B* **1993**, *15*, 199; c) S. Hulth, R. C. Aller, P. Engstrom, E. Selander, *Limnol. Oceanogr.* **2002**, *47*, 212; d) A. Lobnik, I. Oehme, I. Murkovic, O. S. Wolfbeis, *Anal. Chim. Acta* **1998**, *367*, 159.

[27] M. Kerim, A. Gattás, C. L. Stabler, *Biomacromolecules* **2009**, *10*, 3122.

[28] a) E. Wang, K. F. Chow, V. Kwan, T. Chin, C. Wong, A. Bocarsly, *Anal. Chim. Acta* **2003**, *495*, *45*; b) A. Lobnik, I. Oehme, I. Murkovic, O. S. Wolfbeis, *Anal. Chim. Acta* **1998**, *367*, 159; c) M. Cajlakovic, A. Lobnik, T. Werner, *Anal. Chim. Acta* **2002**, *455*, 207; d) C. A. Browne, D. H. Tarrant, M. S. Otleanu, J. W. Mullens, E. L. Chronister, *Anal. Chem.* **1996**, *68*, 2289; e) L. M. Shamansky, M. Yang, M. Olteanu, E. L. Chronister, *Mater. Lett.* **1996**, *26*, 113.

[29] J. D. Malhotra, L. H. Chen, *J. Phys. Chem. B* **2005**, *109*, 3873.

[30] a) J. Choi, M. F. Rubner, *Macromolecules* **2005**, *38*, 116; b) K. Itano, J. Choi, M. F. Rubner, *Macromolecules* **2005**, *38*, 3450. c) R. Kugler, J. Schmitt, W. Knoll, *Macromol. Chem. Phys.* **2002**, *203*, 413; d) J. D. Mendelsohn, C. J. Barrett, V. V. Chan, A. J. Pal, A. M. Mayes, M. F. Rubner, *Langmuir* **2000**, *16*, 5017; e) A. H. Jeri, M. F. Rubner, *Macromolecules* **2003**, *36*, 4078.

[31] P. P. Bontchev, S. Liu, J. L. Krumhansl, J. Voigt, *Chem. Mater.* **2003**, *15*, 3669.

[32] K. Kanamura, J. Hanagami, *Solid State Ionics* **2004**, *172*, 303.